Proceedings World Geothermal Congress 2015
Melbourne, Australia, 19-25 April 2015

Gravity Analysis for Hidden Geothermal System in Cipanas, Tasikmalaya Regency, West Java

Rocky Martakusumah[1,2], Wahyu Srigutomo[1] Suryantini[2], Angga Bakti Pratama[1,2], Trimadona[1] and Arie Haans[3]

[1] Physics of Earth and Complex System Research Division, Bandung Institute of Technology, Bandung 40132, Indonesia

[2] Study Program of Geothermal Engineering, Bandung Institute of Technology, Bandung 40132, Indonesia

[3] PT. Ametis Energy Nusantara, Jakarta 12950, Indonesia

rocky07042@gmail.com

Keywords: Geological Lineament, Heat Source, Inversion Modeling, Gradient Analysis

ABSTRACT

Cipanas Geothermal Prospect in Tasikmalaya Regency is classified as a hidden geothermal system, thus gravity surveying plays an important role in early stage of subsurface imaging. In total, 70 gravity stations have been observed with 1.5-2 km spacing grid within a 15 x 15 km area coverage using a LaCoste-Romberg G-series gravimeter. An integrated gravity interpretation, including horizontal and vertical gradient analysis, and 3-D inversion modeling are provided in this study to recover geological features that occurs on the geothermal system. With the results, we could estimate the location and depth of heat sources and deep geological lineaments that control the Cipanas Geothermal Prospect.

1. INTRODUCTION

The main concern for Cipanas Geothermal Prospect exploration stage is to identify geothermal system components within the hidden geothermal system. It has only one surface manifestation, as a hotspring, that exists today within an area of 15 x 15 km wide. So that, geophysical methods play an important role in reconnaissance surveys to support geology and geochemistry exploration since it could attempt to provide the subsurface imaging based on the measurement on the earth's surface.

The gravity method become an important choice to many problems that involves subsurface mapping, especially in high terrain environments as can be found in common geothermal fields in Indonesia. This is possible due to a good measurement precision level (up to 0.01 mGal), faster measurement and fully portable instrument. Gravity surveying could take a part in identifying the intrusive bodies and major faults that are associated with heat sources and permeability structures of geothermal prospects, respectively. The ability to identify the variations in the gravity field caused by horizontal variations of density within the subsurface is provided by precisely measuring the acceleration of gravity in the vertical direction for each observed station. That high sensitivity is achieved by observing the spring balances in which the change in length of the spring is caused by a change in gravitational attraction.

Therefore, in terms of geophysical reconnaissance survey for Cipanas Geothermal Prospect identification, we proposed to conduct gravity surveying in a more detailed manner (165 observed stations and 1.5 - 2 km spacing grid within 25 km x 27 km area coverage) despite we only provide the interpretation of 70 observed data within 15 x 15 km study area, then analyse this data to discover two geothermal components: the intrusive bodies as heat source and major faults that could control the geothermal system.

In this study we present regional-residual separation using trend surface analysis to isolate the interesting anomalous, horizontal and vertical gradient analysis to locate the boundaries of density contrasts. Moreover, we provide 3-D gravity inversion modeling to obtain more information about geometry of any anomalous body that are associated to geological subsurface structures at Cipanas Geothermal Prospect.

2. GEOLOGY OF STUDY AREA

The Cipanas Geothermal Prospect area is located in West Java Province occupying an area of 15 km x 15 km. It is mostly covered by products of an active volcano in the southern Talaga-Bodas volcano. The geology of the study area where is located in the southern part of Galunggung Volcano had been described by Bronto (1989). The volcano covers an area of 275 km^2 and is bordered by Quaternary volcanoes on the east, north and west sides and Tertiary rocks in the south.

The physiographic of Galunggung area is divided into an Old Galunggung volcanic cone (altitude of 2168 m), a horseshoe-shaped caldera and a hilly area. There is an active crater inside the caldera which has a circular form, approximately 1000 m wide and 150 m deep, where an inactive circular crater exist in the northern side approximately 500 m across and 100 – 150 m deep.

Galunggung Volcano was built on a basement of Permo-Triassic metamorphic rocks, Cretaceous granites, Tertiary volcanic and sedimentary rocks (Bronto, 1989). The oldest rocks (Cretaceous - Eocene age) in West Java area consists of sedimentary rocks and metamorphosed basic such as gabbros and pillow lavas. Meanwhile, the Tertiary volcanic rocks are basalts at the top part, andesites in the middle part and dacites in the lower part.

Galunggung volcanic rocks could be divided into Old Galunggung Formation, Tasikmalaya Formation and Cibanjaran Formation. The regional tectonic activity is one of the important parameters that triggered the Galunggung eruption (Bronto, 1989). Old Galunggung volcano is classified as a stratovolcano which consists of lava flows, pyroclastic flows, pyroclastic falls and lahars with a total rock volume at about 56.5 km3. The eruption processes finally yields a horseshoe-shaped caldera and ejected more than 20

km^3 of material that consists of debris avalanche, pyroclastic flow, pyroclastic fall, pyroclastic surge and lahar deposits. Historic eruptions are separated by long dormant periods and produced volume is about less than 0.4 km^3 and comprising debris avalanche, pyroclastic flow, pyroclastic fall, pyroclastic surge, lava and lahar deposits (Bronto, 1989).

3. GRAVITY DATA

The acquisition of land gravity data has been carried out in 165 observed stations with a 2 km spacing grid within a 25 x 17 km area coverage (Figure 1). However, for certain reason, this study only presents 70 observed points that covers an area of 15 x 15 km within the black-line boundary in Figure 1. The data reduction process has been carried out by removing the temporal and spatial effects contained in each raw data. The step-by-step of our gravity reduction is clearly shown in Figure 2. The Bouguer density was determined mathematically using the Parasnis method. It is a plot that correlates the Bouguer anomaly and topography factor (Yamamoto, 1999). The *(0.04185*h)-Tc* is plotted against $(G_{obs}-G_n+0.3086h)$ and the slope of the straight line is adopted as the estimated Bouger density value that will be used in the complete Bouguer anomaly calculation. Figure 3 shows that the Bouguer density value is 2.66 gr/cc.

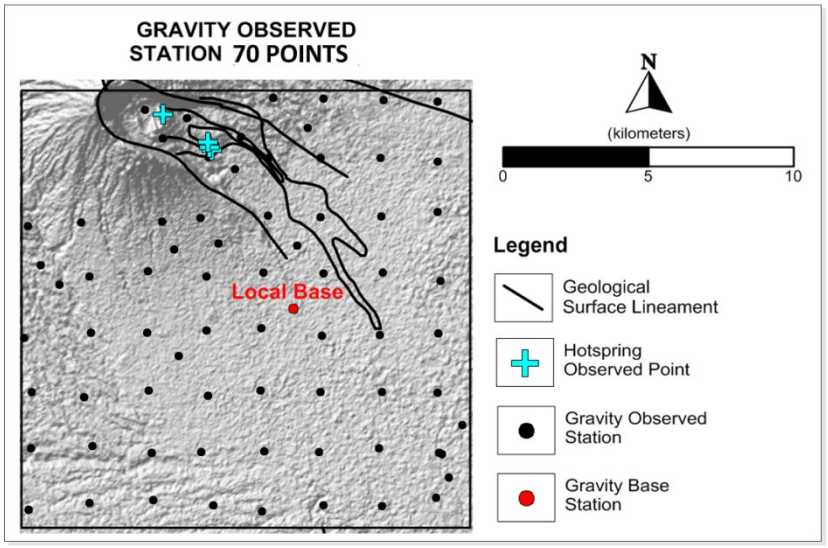

Figure 1: Map location of gravity observed stations.

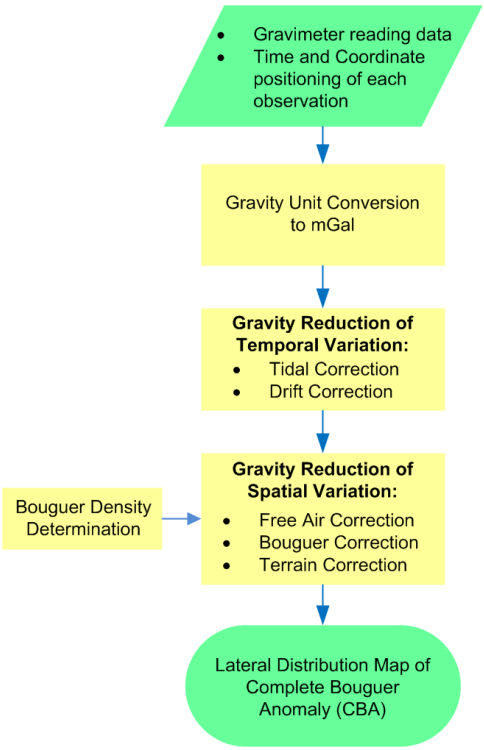

Figure 2: Flowchart of gravity data reduction.

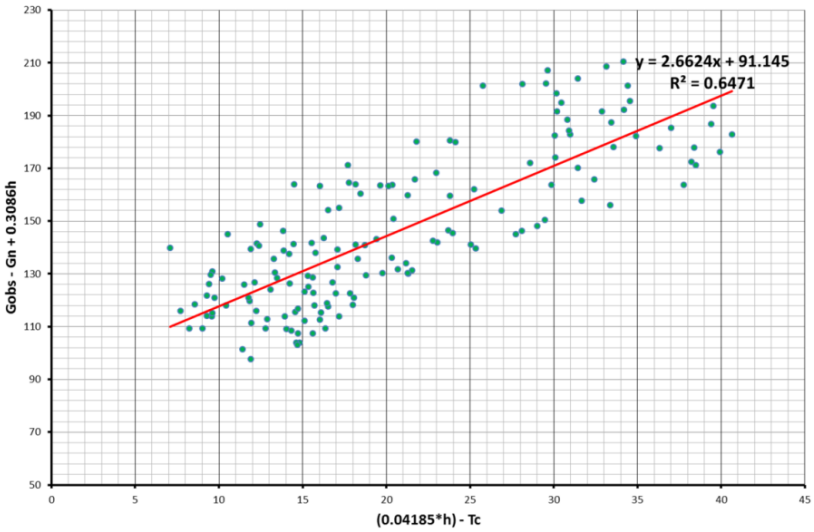

Figure 3: Results of Parasnis method for Bouguer density estimation.

4. ANALYSIS AND INTERPRETATION

4.1 Regional – Residual Separation

Figure 4 shows the complete Bouguer anomaly (CBA) gridded contour map for the survey area. Its range is between 25-100 mGals and contains information about superposed anomalies from the several sources beneath the subsurface. First, we attempted to figure out the longer-wavelength features that must be associated with deep density contrasts by performing a first-order regional anomaly contour map as shown in Figure 5. The result was confirmed by the regional geology map of the area and well suited to the geological standpoint. The low anomaly in the north is evidence of a Quaternary volcanic zone, whereas the high anomaly might reflect the Tertiary zone. It explains why any subsurface material that remains buried for a long time is consolidated and compacted, resulting in reduced porosity and increasing the density.

Residual anomaly contour maps were provided to observe the shorter-wavelength anomalies that arose from shallower geological features (Kearey, 2002). This step removed the regional anomaly from CBA and left the local anomalies with possible control on the investigated geothermal system. In our study, these values were produced by subtracting the CBA data by the first-order regional data, as can be seen in Figure 6. In general, it shows a significant high anomaly (amplitude > 15 mGals) in the northern part of the study area, which is exactly underneath the active volcano. Its existence is interpreted as the possibility of a intrusive body, as we know that plutonic rocks tend to be denser than their volcanic equivalents. Moreover, it might be related to the geothermal heat source(s).

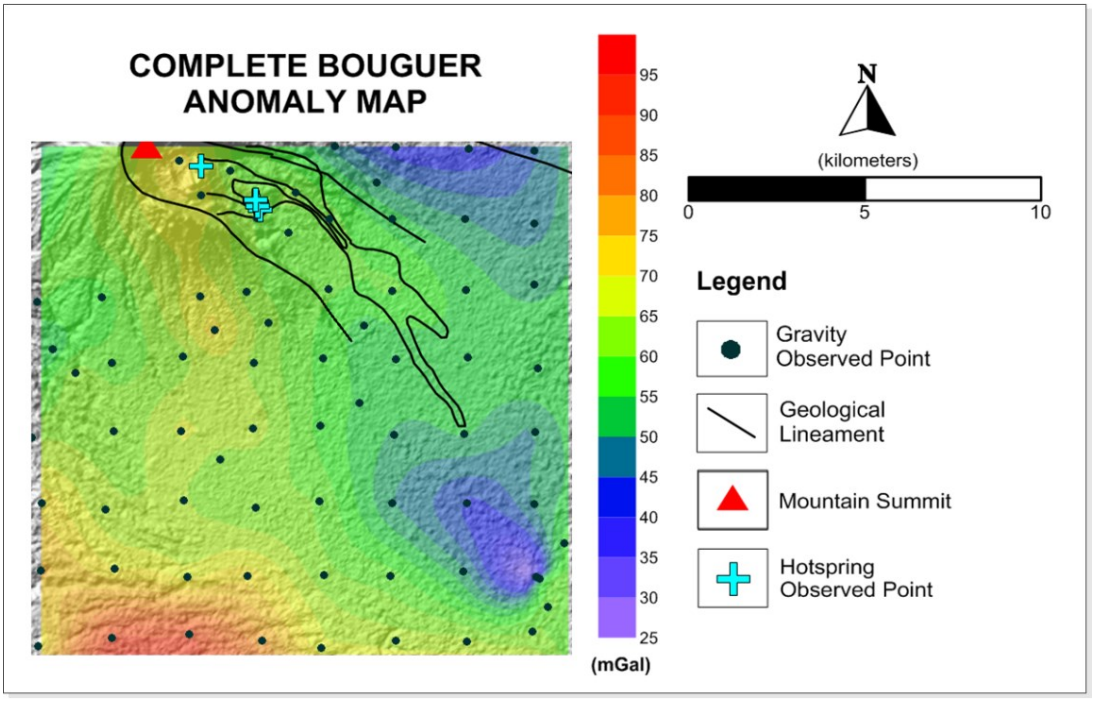

Figure 4: Complete Bouguer anomaly map of the survey area.

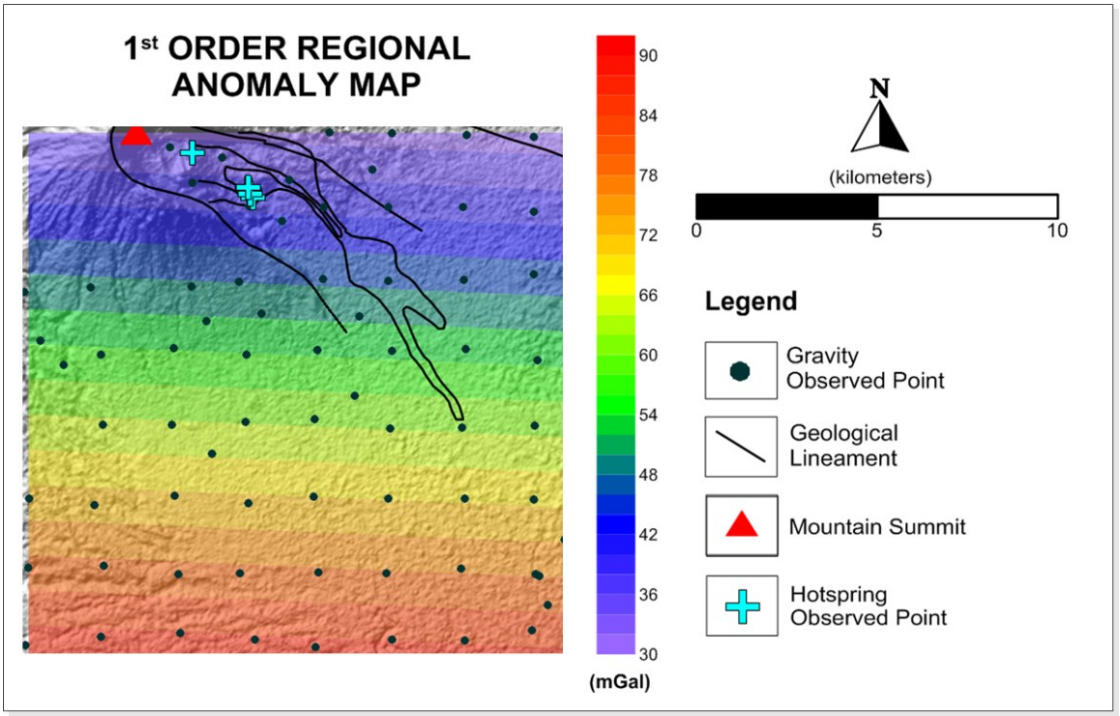

Figure 5: Regional anomaly contour map generated by first order polynomial technique.

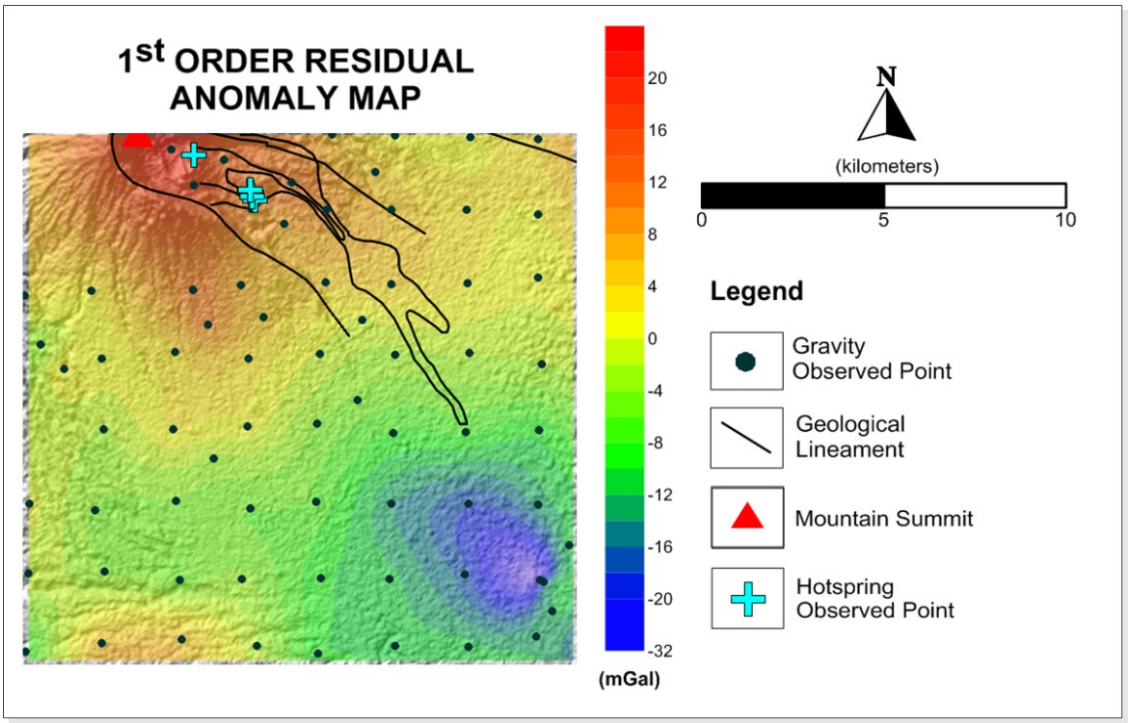

Figure 6: Residual anomaly map generated by removing first order polynomial surface.

4.2 Gradient Analysis

We obtained three horizontal gradient contour maps in total from the observed CBA data which are the horizontal derivative in the x direction, y direction and the resultant itself. They were carried out to locate the lateral boundaries of density contrasts that related to any relatively deep faults or geological boundaries within the subsurface (Saibi, 2006).

The horizontal derivative in x direction is defined as the rate of change of observed CBA data with respect to x. Hence, it measures the slope or gradient of the observed CBA data in x direction and consequently emphasizing the north-south lineaments. Figure 7 obviously shows a significant horizontal gradient anomaly that lies on the north-south orientation across the survey area. Its appearance might be presumed as a deep fault or lithological contact within the subsurface and must be investigated in more detail whether it is potential as a geothermal reservoir(s) or not.

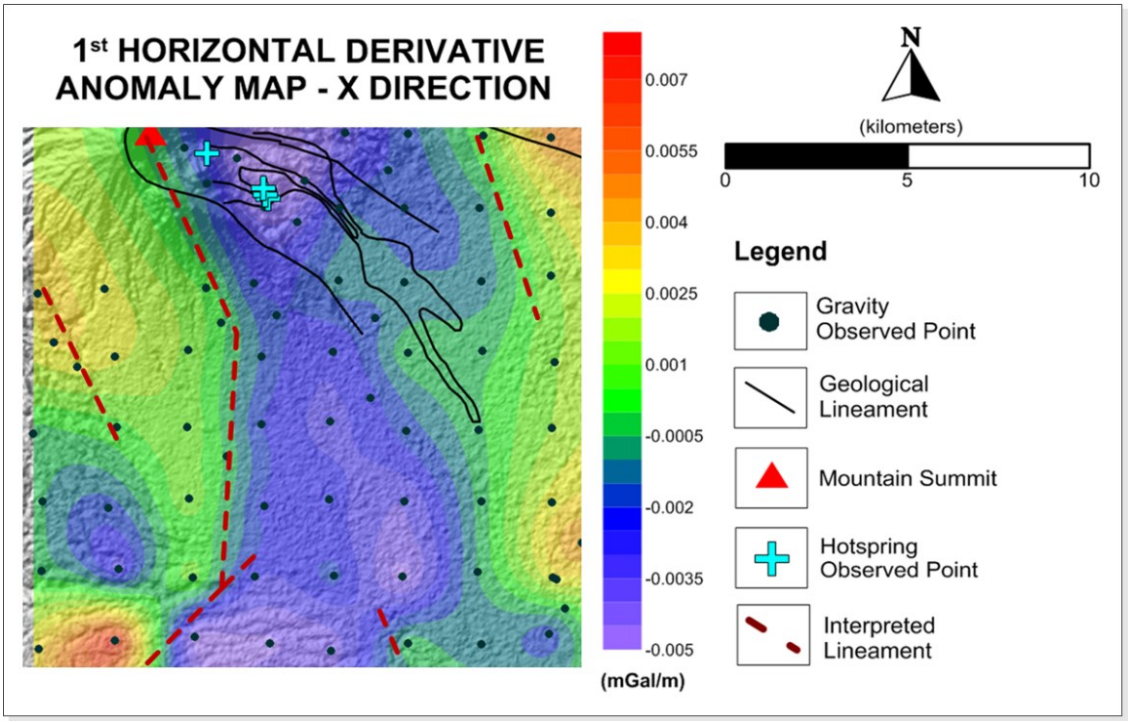

Figure 7: Map showing the first-order horizontal derivative anomaly in x direction.

Conversely, the horizontal derivative in y direction is defined as the rate of change of observed CBA data with respect to y. Figure 8 shows several horizontal gradient anomalies that lie on a west-east orientation across the survey area. The map shows that the most significant west-east gradient anomaly lies on the northern part of survey area. Such anomaly might reflect a deep lithological contact and could be presumed as the northern boundary of the investigated geothermal area.

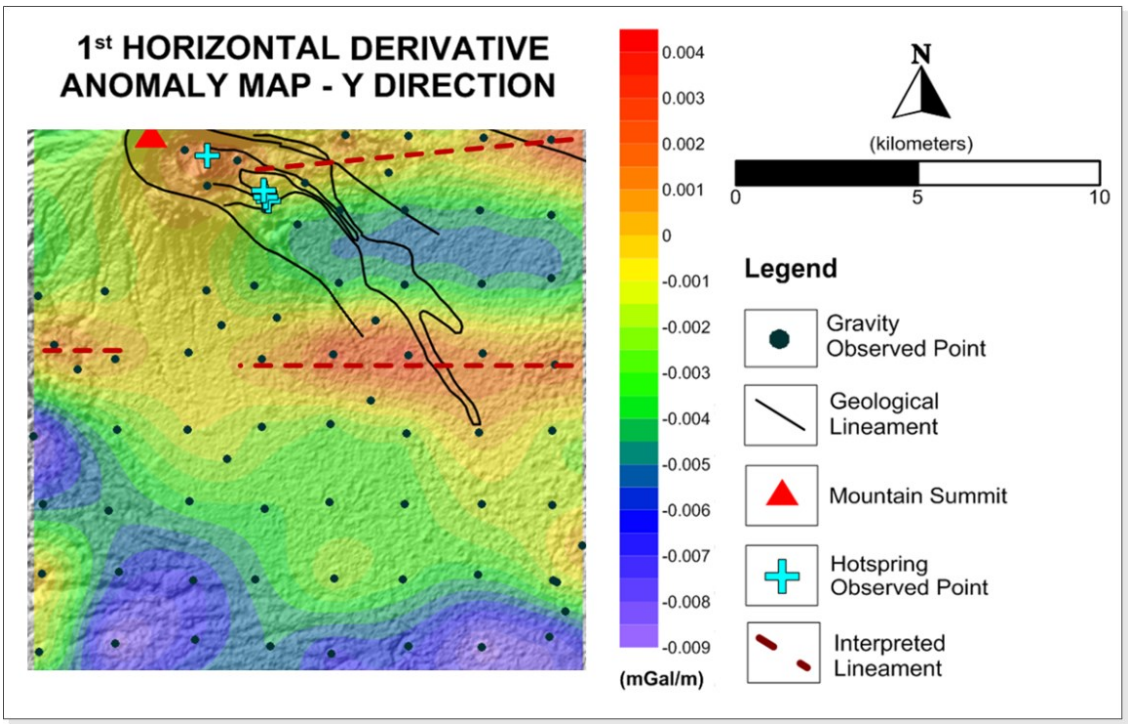

Figure 8: Map showing the first-order horizontal derivative anomaly in y direction.

The total horizontal derivative map is shown in Figure 9 which is the square root of the sum of squared x and y horizontal derivatives. The map indicates the complexity of the anomaly boundaries, which are caused by several boundary orientations. Hence, the pattern of high gradient anomalies is broader and less sharp.

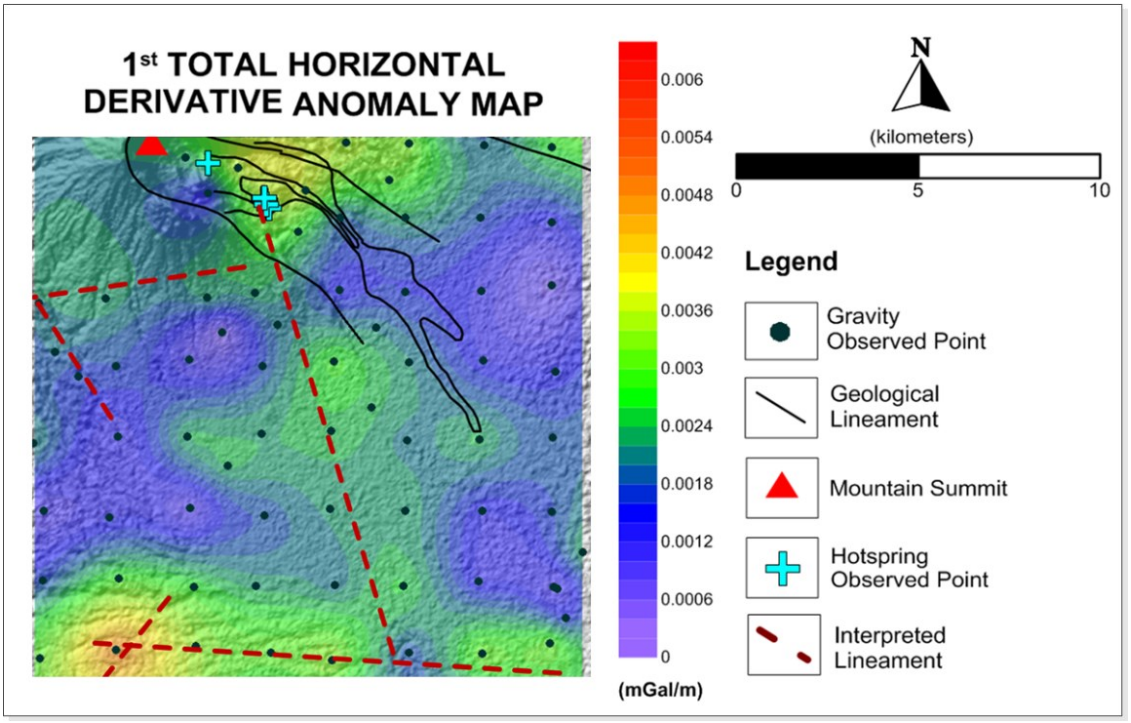

Figure 9: Map showing the total horizontal derivative (resultant) anomaly in y direction.

The first vertical derivative has been applied to the CBA data to reveal the vertical boundaries of density contrasts. Figure 10 shows the study area which is dominated by medium-high gradient amplitudes. It indicates the significant rate of change of gravity vertically from low density to higher densities, and vice versa. Meanwhile, the low gradient amplitude could be found exactly beneath the volcano's cone which might correspond to a massive intrusive body.

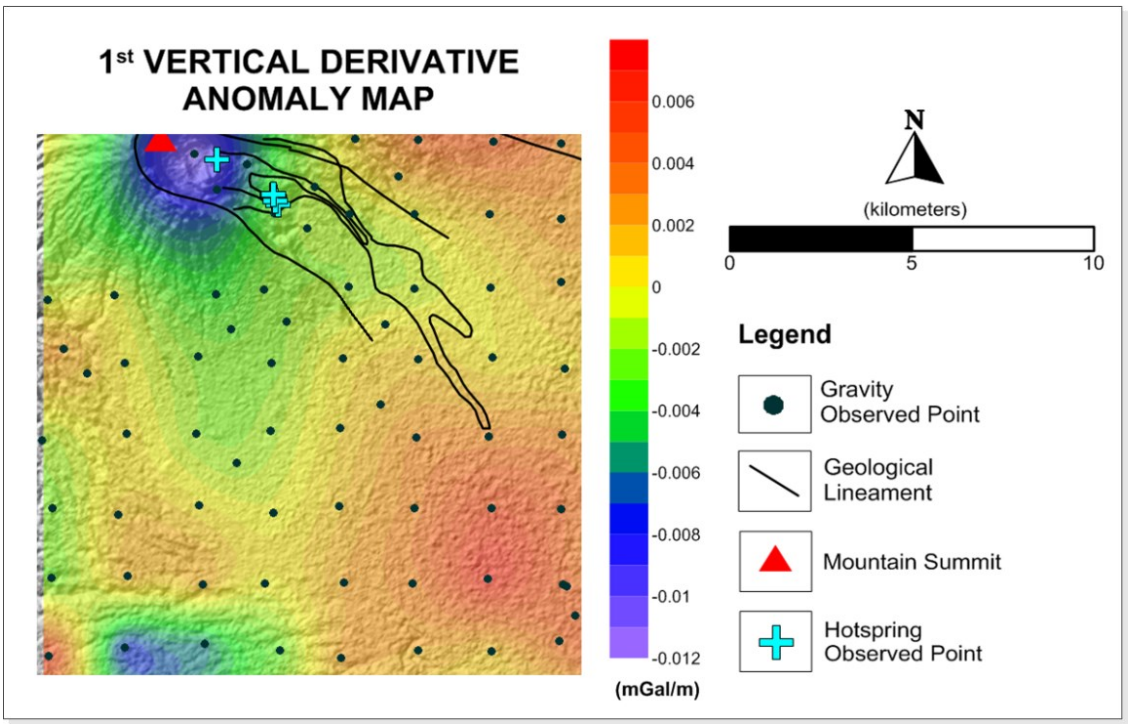

Figure 10: Map showing the first-order vertical derivative anomaly in y direction.

The second vertical derivative (SVD) has been provided as a second opinion to remove the effect of the regional field from CBA data, hence emphasizes the local anomalies related to shallow structures. Unfortunately, SVD also amplifies noise, which could produce many second-derivative anomalies that are not related to geology (Reynolds, 1997). Figure 11 tends to locate a high anomaly closure underneath the volcano in the northern survey area, in a similar position to the one determined by trend surface analysis. Therefore, it could support our previous interpretation about the presence of an intrusive body underneath the volcano.

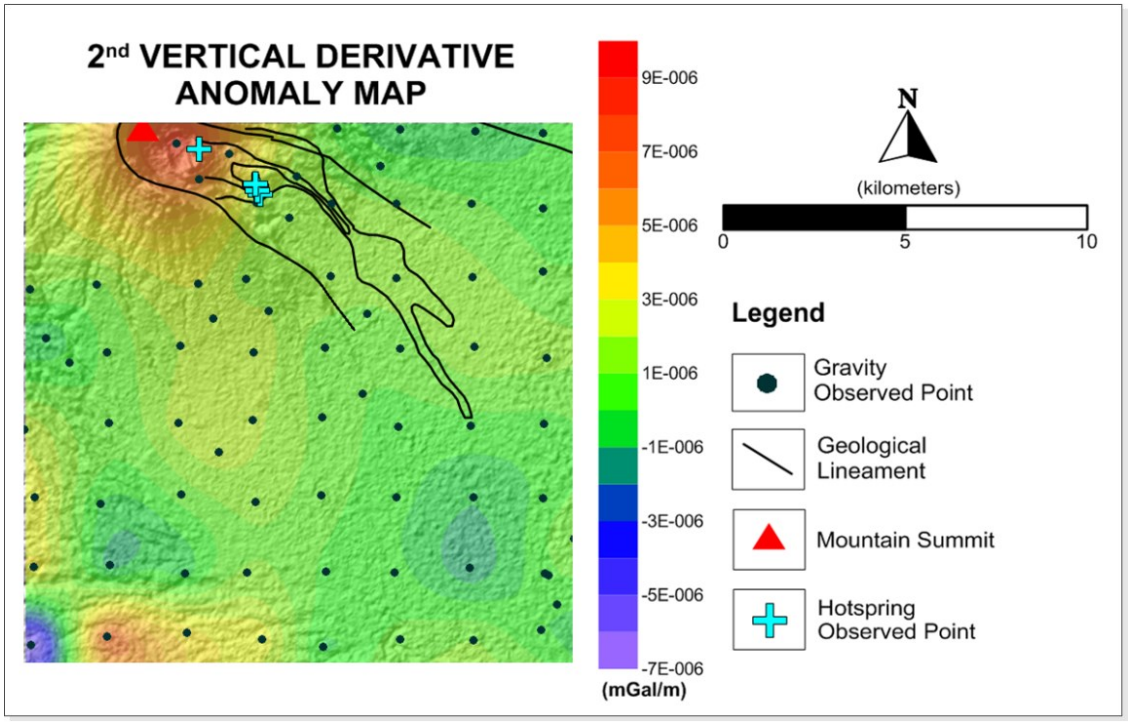

Figure 11: Map showing the second-order vertical derivative anomaly in y direction.

Figure 12 shows the integrated interpretation of geological structures from the gradient analysis. The SVD analysis indicates the potential location of the heat source beneath the volcano, whereas the horizontal gradient shows several trends of fault zones and/or lithological contacts. The lineament I in Figure 12, which is identified as a structure between two mountains by horizontal derivative in x-direction and the total horizontal derivative should be observed in detail whether it is potential as a permeability structure(s). It is presumed to occur in relatively deep underneath the earth's surface. Meanwhile the occurrence of hot spring near the caldera is presumed to emerge from the lineament II which has an N – S orientation, thus also might be identified as the other permeability structure(s) underneath the surface within our study area. Moreover, we conclude that the specified geothermal prospect area is covered within the black dashed-line boundary in Figure 12.

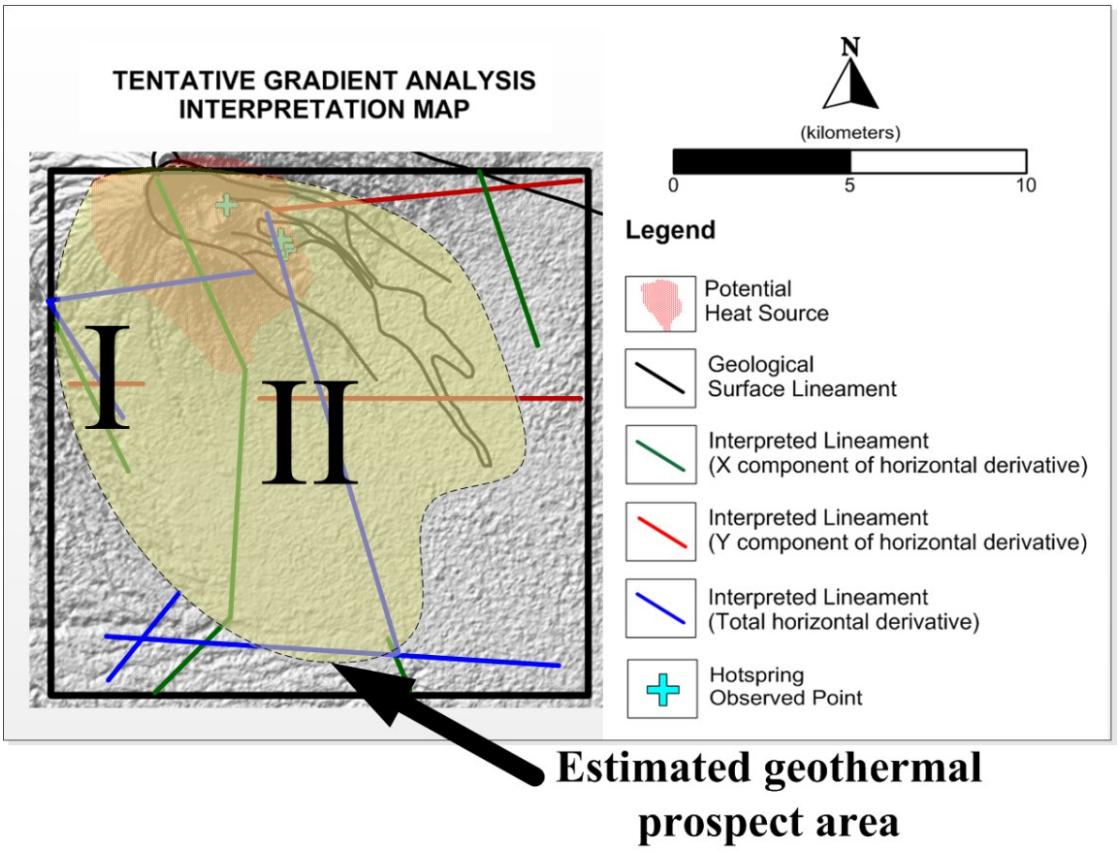

Figure 12: Map showing the integrated deep structures interpretation.

4.3 Three-Dimensional Inversion Modeling

To delineate the three dimensional shape of the anomalous density body associated with the heat source(s), we present a 3-D gravity inversion modeling which has been adopted from Li and Oldenburg (1998) by the GRAV3D program. The three dimensional density contrast distribution has been estimated by a 3-D model that fits the observed residual data.

The inversion was performed within a 25 x 27 km area and depth of about 5 km. The 3-D model mesh, which is constructed by 108,000 cells, has been designed in accordance with the area of interest and the spacing of the observed data that covers the area. It consists of 60 x 60 x 30 cells where each cell is 418 m by 447 m by 208 m. Digital Elevation Model (DEM) data has been used to define the surface topography of the 3-D model. Therefore the cells above the topographic surface are simply removed from the visualized three-dimensional density contrast model.

Figure 13 shows the recovered 3-D density contrast model for the study area. The model is characterized by a minimum density contrast of -0.5 gr/cc and maximum value of 0.5 gr/cc with the reference model of 2.67 gr/cc. Figure 13 shows the interpreted N-S cross-section cut through Galunggung volcano southward at the observation area. On this figure, we could observe a positive density contrast that shaped intusively right underneath Galunggung volcano, detected under 1900 masl up and bordered by negative density contrast defined as a deflection structure in the southern side. The presence of the deflection structure was later identified from geological surface surveys to be filled by volcanic products resulted from Galunggung volcano eruptions over several periods. Moreover, the recovered 3-D geometry of an intrusive body that might be correlated with a heat source could be seen obviously in Figure 14. This result was obtained by only selecting positive density contrasts higher than 0.3 gr/cc, which was defined to be density characteristic values for igneous rocks such as gabbro and diorite.

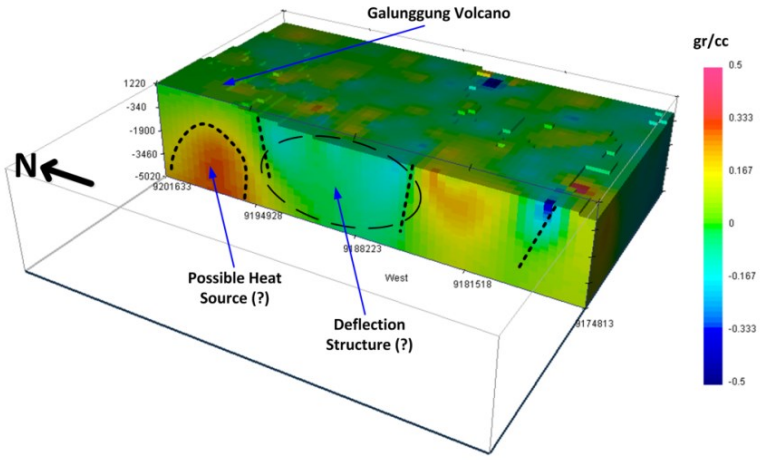

Figure 13: Inverted model section from 3-D gravity modeling.

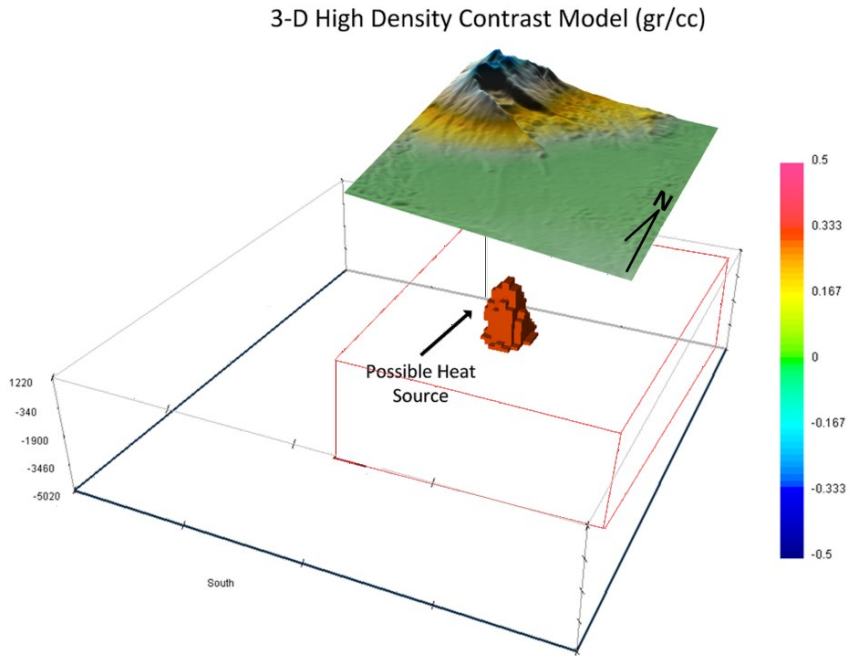

Figure 14: Recovered 3-D high density contrast.

5. CONCLUSIONS

In this type of Indonesia's geothermal green field we attempted to provide the identification of lateral faults distribution, intrusive bodies and preliminary estimation of its depth. The combination of horizontal gradient analysis in x direction, y direction, and the resultant itself yield the existence of subsurface geological lineaments (e.g. Lineament I and II) that might be related to any permeability structure. These results give a new fact about the occurrence of any lineaments that had not been revealed on the surface. For future works, the Euler deconvolution analysis could be provided to infer the depth.

The 3-D gravity inversion modeling has been presented to delineate the three dimensional shape of the gravity anomaly associated with the heat source(s) of Cipanas Geothermal Prospect. It delineates an intrusive body beneath the Galunggung volcano with density contrasts higher than 0.3 gr/cc, which was defined to be density characteristic value for igneous rocks such as gabbro and diorite. In addition, magnetotelluric surveys could be considered to cover the estimated geothermal prospect area that has been delineated by our gravity analysis.

ACKNOWLEDGEMENT

We would like to thank Energy Kinan Internasional, Ametis Energy Nusantara and LAPI ITB for providing the complete gravity data. We are also greatly appreciating ITB Postgraduate Program of Geothermal Engineering and ITB Earth Physics Laboratory for their contribution and support during this work.

REFERENCES

Bronto, Sutikno. 1989. *Volcanic Geology of Galunggung, West Java, Indonesia*. Thesis, Geology, University of Canterbury.

Kearey, Philip. 2002. *An Introduction to Geophysical Exploration*. London: Blackwell Science Ltd.

Reynolds, John M. 1997. *An Introduction to Application and Environmental Geophysics*. West Sussex: John Wiley & Sons Ltd.

Saibi, H., Nishijima, Jun. 2006. *Processing and Interpretation of Gravity Data for the Shimabara Peninsula Area, Southwestern Japan.*Memoirs of the Faculty of Engineering, Kyushu University, Vol. 66, No.2.

Wright, Philip M., dkk. 1985. *State-of-the-art geophysical exploration for geothermal resources*: Geophysics Vol. 50, No.12 P. 2666-2699.

Yamamoto, Akihiko. 1999. *Estimating the Optimum reduction Density for Gravity Anomaly: A Theoretical Overview*. Jour. Fac. Sci., Hokkaido Univ., Ser. VII (Geophysics), Vol. 11 No. 3, 577-599.